

## Preparation and characterization of $\text{Na}_2\text{O}-\text{Al}_2\text{O}_3-\text{B}_2\text{O}_3$ sol-gel glasses with aluminum lactate and formiate as precursors

Lars P. Hoyer, Gundula Hensch and Günther Heinz Frischat

Institut für Nichtmetallische Werkstoffe, Technische Universität Clausthal, Clausthal-Zellerfeld (Germany)

Long Zhang and Hellmut Eckert

Institut für Physikalische Chemie, Westfälische Wilhelms-Universität, Münster (Germany)

---

In this work aluminum lactate and aluminum formiate have been used as precursors to obtain room temperature stable sols and gels and after annealing homogeneous glasses in the system  $\text{Na}_2\text{O}-\text{Al}_2\text{O}_3-\text{B}_2\text{O}_3$ . The local environments and connectivities of boron and aluminum have been investigated by  $^{11}\text{B}$  and  $^{27}\text{Al}$  solid-state nuclear magnetic resonance (NMR). It was found that the local atomic structures of the sol-gel glasses markedly depend on the precursors and the preparation routes and are also dissimilar to those of melt quenched glasses of the same compositions. Thus, for example, the fractions of  $\text{BO}_{3/2}$  and  $\text{BO}_{4/2}$  units differ and it is interesting to note that there are no asymmetric  $\text{BO}_{2/2}(\text{O}^-)$  units present in the sol-gel materials. The  $^{27}\text{Al}$  spectra show Al in four-, five- and sixfold coordination, whose relative abundance in a given glass composition is also dependent on the preparation route. Rotational echo double resonance (REDOR)  $^{11}\text{B}$   $\{^{27}\text{Al}\}$  and  $^{27}\text{Al}$   $\{^{11}\text{B}\}$  results indicate that the extent of B–O–Al connectivity is diminished in the gel prepared glasses when compared to the melt cooled glasses. Element distributions are reported on the basis of secondary neutral mass spectrometry (SNMS) data, and the nanostructures of surfaces have been characterized by atomic force microscopy (AFM).

---

### 1. Introduction

While the sol-gel technique is well established for the preparation of stable silicate-based glasses [1 and 2], its application to multicomponent nonsiliceous systems is still in the beginning. Such glasses are of interest for various applications in the optics and coating fields. Because of favourable mechanical and optical properties the sodium-aluminoborate ( $\text{Na}_2\text{O}-\text{Al}_2\text{O}_3-\text{B}_2\text{O}_3$ , NAB) glass system is an attractive candidate for the development of a new sol-gel methodology. In recent work the successful sol-gel preparation of glasses in the  $\text{Na}_2\text{O}-\text{Al}_2\text{O}_3-\text{P}_2\text{O}_5$ ,  $\text{Al}_2\text{O}_3-\text{P}_2\text{O}_5$ , and  $\text{Na}_2\text{O}-\text{AlPO}_4$  systems was achieved by using aluminum lactate as a precursor species [3 to 5]. Thus, for example, the preparation of glasses became feasible also in the  $\text{Na}_2\text{O}-\text{AlPO}_4$  system, where a melt-based formation has not been possible yet [5]. On the other hand it could be shown by  $^{27}\text{Al}$  and  $^{31}\text{P}$  nuclear magnetic resonance (NMR) that the structures of sol-gel formed and melt quenched  $\text{Na}_2\text{O}-\text{Al}_2\text{O}_3-\text{P}_2\text{O}_5$  [3] and  $\text{Al}_2\text{O}_3-\text{P}_2\text{O}_5$  [4] glasses are the same at a given composition, which means that the structures of these materials do not depend on the specific prep-

aration route. In the present contribution we demonstrate both the use of aluminum lactate and aluminum formiate precursors for preparing sol-gel glasses in the NAB system. Various glass compositions have been prepared and compared to corresponding preparations via the melt cooling route [6 and 7]. Using  $^{11}\text{B}$  and  $^{27}\text{Al}$  solid-state NMR techniques it will be demonstrated that the network structures of these sol-gel glasses are quite different and also different from those of melt prepared glasses with the same chemical compositions. We also report data concerning the preparation of thick films, the drying of the gels, and the elemental homogeneity of the glasses using secondary neutral mass spectrometry (SNMS). Finally, the nanostructures of surfaces have been investigated by atomic force microscopy (AFM).

### 2. Experimental

#### 2.1 Preparation of the precursor solutions

Figure 1 displays the flow scheme for the preparation of the lactate containing precursor solution. Starting with a 10 % solution of boric acid,  $\text{H}_3\text{BO}_3$  (Riedel de Haën, pur.) in acetic anhydride  $(\text{CH}_3\text{CO})_2\text{O}$  (Merck, pur.), containing small amounts of formamide,  $\text{H}(\text{CO})\text{NH}_2$  (Merck, puriss.), aluminum lactate  $\text{Al}(\text{CH}_3\text{CH}(\text{OH})\text{COO})_3$  (Fluka, pur.) and

---

Received 31 May 2005.

Presented in German at 77<sup>th</sup> Annual Meeting of the German Society of Glass Technology (DGG) in Leipzig (Germany) on 27 May 2003.

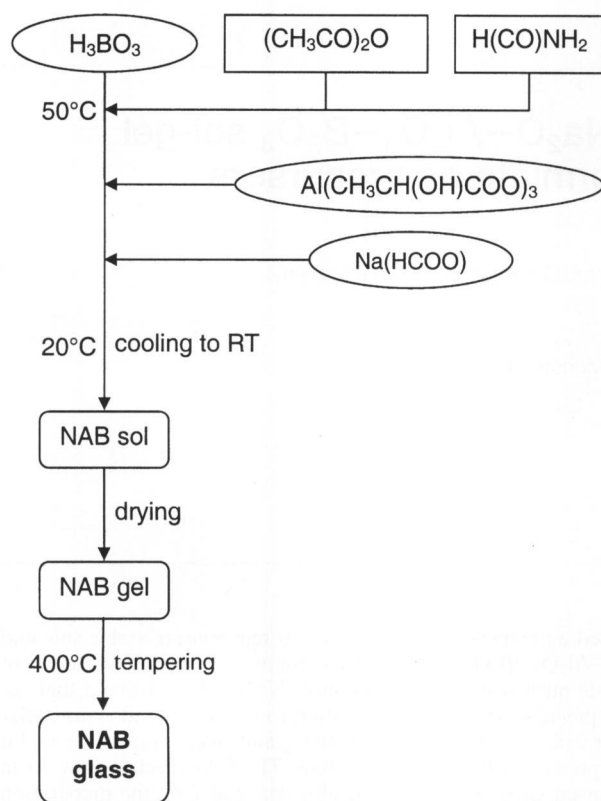


Figure 1. Flow scheme for the preparation of the precursor solution with aluminum lactate and the resulting  $\text{Na}_2\text{O}-\text{Al}_2\text{O}_3-\text{B}_2\text{O}_3$  glass.

sodium formiate  $\text{Na}(\text{HCOO})$  (ABCR, pur.) were added according to the compositions shown in table 1. To dissolve the boric acid in acetic anhydride the mixture had to be stirred at  $50^\circ\text{C}$  and the formamide was added increasing with the final sodium content of 25 to 55 mol%  $\text{Na}_2\text{O}$  in steps of 0.25 % per 5 mol%  $\text{Na}_2\text{O}$ . While quickly stirring this solution, the required amount of aluminum lactate was added in small portions. After it was dissolved completely within some minutes, the required amount of sodium formiate was added at once. Subsequently the sol was stirred for another 30 min at  $50^\circ\text{C}$  to ensure that it is homogeneous and stable, and can be cooled to room temperature without

crystallization. It looks yellow, and bulk solutions form gels within several days, while thick films on a glass substrate exhibit gellation within a few minutes.

Figure 2 displays the flow scheme for the preparation of the formiate containing precursor solution. Aluminum nitrate nonahydrate,  $\text{Al}(\text{NO}_3)_3 \cdot 9\text{H}_2\text{O}$  (Riedel de Haën, pur.), was dissolved in distilled water, stirring the solution while adding 1 mol/l  $\text{NaOH}$  which leads to the precipitation of aluminum hydroxide,  $\text{Al}(\text{OH})_3$ . Aluminum formiate,  $\text{Al}(\text{HCOO})_3$ , was produced by dissolving this aluminum hydroxide in formic acid,  $\text{HCOOH}$  (98 to 100 %, Merck, pur.). In this solution boric acid  $\text{H}_3\text{BO}_3$  (> 98.8 %, Riedel de Haën, pur.) and the sodium formiate,  $\text{Na}(\text{HCOO})$  (> 98 %, ABCR) were dissolved at  $\approx 40^\circ\text{C}$  according to the compositions shown in table 2. The resulting sol is stable only at higher temperature; during cooling boric acid crystallizes.

## 2.2 Thick film preparation

Thick films (0.1 to 0.3 mm) were prepared by dip coating silica glass substrates with the pre-gelled solutions or by pouring the solution into glass or ceramic dishes. We used Petri dishes, which were filled with about 2 mm of the previously prepared sols. In the lactate case the films were dried at temperatures up to  $80^\circ\text{C}$ , applying a low vacuum to facilitate solvent evaporation. Drying at higher temperatures leads to formation of bubbles and/or foam while drying. After this initial drying step, which removes most of the solvent, a second drying step at lower temperatures and ambient humidity condition was found to lead to a better removal of the organics. The acetic anhydride reacts with the humidity to acetic acid which probably protonates the lactate to lactic acid but not the formiate (higher acid strength than acetic acid) inserted with the sodium. Now the lactic acid and the excess of acetic acid are mobile and can be removed from the gel while the remainder of acetate and all the formiate can be oxidized easily at a subsequent annealing stage. The resulting films are transparent, sometimes light yellow. Annealing the dried gels for 2 h at 130 to  $150^\circ\text{C}$  and for another hour at  $400^\circ\text{C}$  results in the formation of transparent glasses.

In the formiate case drying is performed best by quickly treating about 0.2 mm thick layers in an air flow, where the

Table 1. Characteristic simulation parameters of the  $^{11}\text{B}$  MAS-NMR spectra of the sol-gel glasses (see figure 3) with aluminum lactate as precursor species;  $\delta_{\text{iso}}$ : isotropic resonance shift,  $N_4/N_3$ : percentage of  $\text{BO}_4/\text{BO}_3$  units,  $C_Q$ : quadrupolar coupling constant,  $\eta$ : asymmetry parameter,  $s$ : standard deviation

glass	$\text{Na}_2\text{O}$ in mol%	$\text{Al}_2\text{O}_3$ in mol%	$\text{B}_2\text{O}_3$ in mol%	$\text{BO}_4$		$\text{BO}_3$		$C_Q$ in MHz $s: \pm 0.05$	$\eta$ $s: \pm 0.1$
				$\delta_{\text{iso}}$ in ppm $s: \pm 0.2$	$N_4$ in % $s: \pm 1.5$	$\delta_{\text{iso}}$ in ppm $s: \pm 0.6$	$N_3$ in % $s: \pm 2.5$		
NAB03	25	20	55	1.9	1.5	18.6	98.5	2.76	0.1
NAB07	30	20	50	1.9	2.0	18.4	98.0	2.77	0.1
NAB09	30	30	40	1.5	2.6	18.5	97.4	2.72	0.12
NAB11	35	10	55	0.8	17.2	18.2	82.8	2.68	0.15
NAB16	38	12	50	0.8	8.5	18.1	91.5	2.75	0.11
NAB18	40	20	40	1.9	3.1	17.9	96.9	2.67	0.05
NAB20	40	30	30	2.1	1.8	18.1	98.2	2.74	0.11
NAB25	50	17	33	1.2	6.7	18.1	93.3	2.69	0
NAB27	55	15	30	1.2	8.0	18.1	92.0	2.69	0

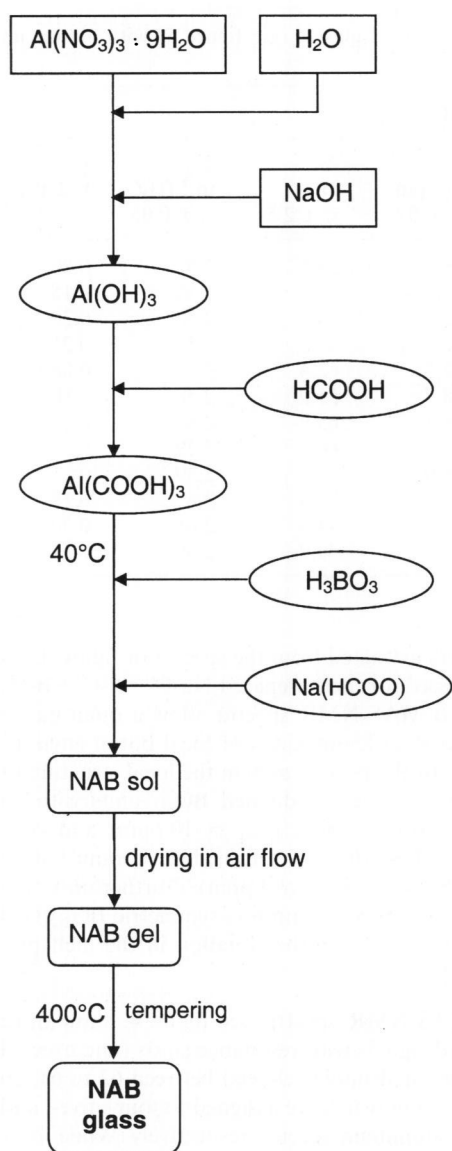


Figure 2. Flow scheme for the preparation of the precursor solution with aluminum formiate and the resulting Na<sub>2</sub>O–Al<sub>2</sub>O<sub>3</sub>–B<sub>2</sub>O<sub>3</sub> glass.

latent heat of evaporation of the solvent reduces the ionic mobility, thus preventing crystallization and/or phase separation. A subsequent annealing for 1 h at 400°C also leads to glass formation.

### 2.3 Methods of characterization

For the solid-state NMR measurements powdered materials obtained by mechanically scratching off the thick films from the Petri dishes were used. The solid-state <sup>11</sup>B and <sup>27</sup>Al NMR experiments were conducted on Bruker DSX-400 and DSX-500 NMR spectrometers equipped with 4 mm MAS NMR probes. Typical operating spinning speeds were 10 to 12 kHz. Spectra were acquired with small flip angles accomplished by short pulses of 1 to 2 μs length. Relaxation delays were chosen to ensure representative spectra. Chemical shifts are reported relative to external standards of BF<sub>3</sub>O(Et)<sub>2</sub> and aqueous 1 mol/l AlCl<sub>3</sub> solution, respectively.

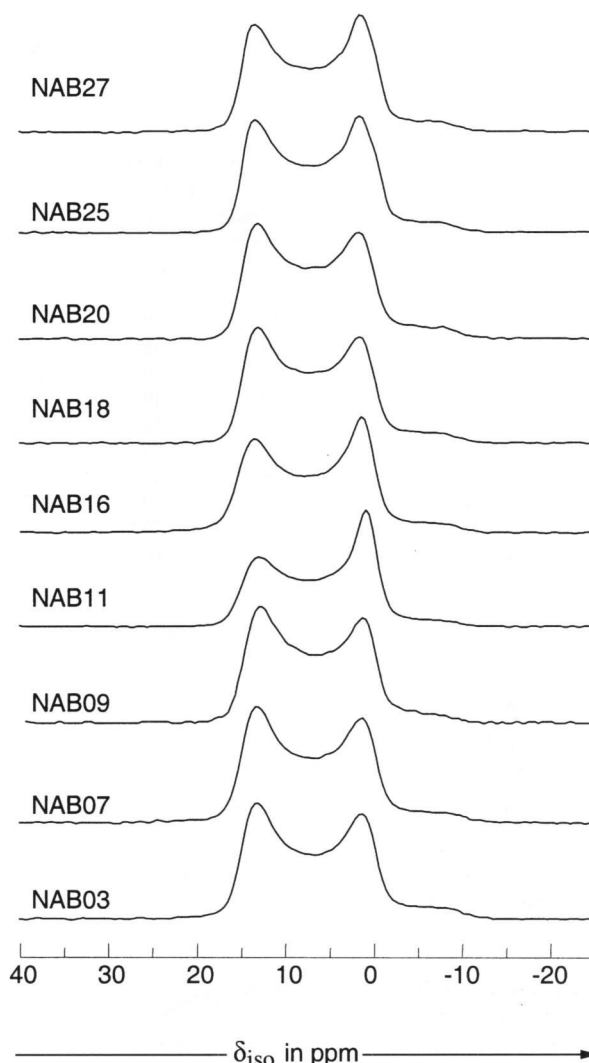


Figure 3. 128.4 MHz <sup>11</sup>B MAS-NMR spectra of the Na<sub>2</sub>O–Al<sub>2</sub>O<sub>3</sub>–B<sub>2</sub>O<sub>3</sub> glasses according to table 1; aluminum lactate as precursor species.

Rotational echo double resonance (REDOR) NMR studies were conducted at a magnetic field strength of 11.7 T (<sup>11</sup>B and <sup>27</sup>Al resonance frequencies of 160.4 and 130.3 MHz, respectively) using similar conditions as those reported in [7]. A dipolar evolution time of 1 ms was used in all cases. The film compositions and their elemental homogeneities were checked by secondary neutral mass spectrometry (SNMS) with a depth resolution of 3 to 5 nm, using a Leybold INA 3 apparatus [8]. The nanostructures of surfaces were inspected by atomic force microscopy (AFM) with a lateral resolution of several nm and a depth resolution of < 0.1 nm, using a Digital Instruments Nanoscope II AFM apparatus [9].

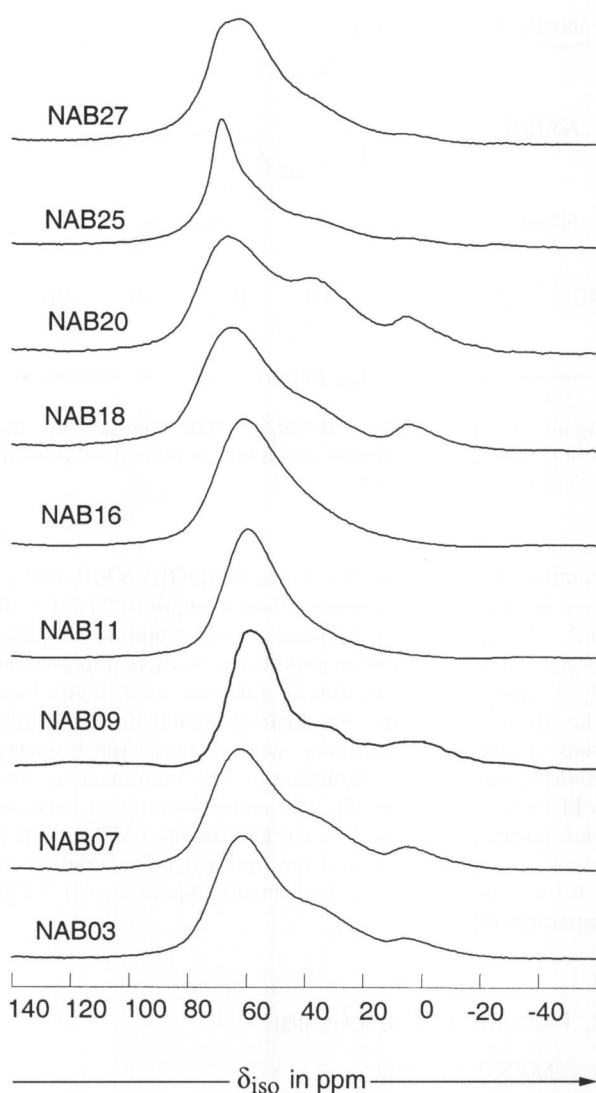
## 3. Results and discussion

### 3.1 MAS-NMR data

Figures 3 and 4 summarize the <sup>11</sup>B and <sup>27</sup>Al MAS-NMR spectra of the aluminum lactate based sol-gel glasses measured in the present study. Table 1 shows the corresponding

Table 2. Characteristic simulation parameters of the  $^{11}\text{B}$  MAS-NMR spectra of the sol-gel glasses (see figure 5) with aluminum formiate as precursor species; for explanation of symbols see table 1

glass	$\text{Na}_2\text{O}$ in mol%	$\text{Al}_2\text{O}_3$ in mol%	$\text{B}_2\text{O}_3$ in mol%	$\text{BO}_4$		$\text{BO}_3$		$C_Q$ in MHZ $s: \pm 0.05$	$\eta$ $s: \pm 0.1$
				$\delta_{\text{iso}}$ in ppm $s: \pm 0.2$	$N_4$ in % $s: \pm 1.5$	$\delta_{\text{iso}}$ in ppm $s: \pm 0.6$	$N_3$ in % $s: \pm 2.5$		
NAB03	25	20	55	1.5	44.5	18.7	55.5	2.53	0.20
NAB07	30	20	50	1.7	38.7	17.8	61.3	2.52	0.15
NAB09	30	30	40	1.8	25.4	18.2	74.6	2.55	0.20
NAB11	35	10	55	1.8	53.8	18.5	46.2	2.53	0.25
NAB16	38	12	50	1.0	34.6	18.5	62.4	2.62	0.08
NAB18	40	20	40	1.5	44.1	18.7	55.9	2.58	0.10
NAB20	40	30	30	1.3	34.1	18.3	65.9	2.65	0
NAB25	50	17	33	1.2	40.0	18.3	60.0	2.59	0
NAB27	55	15	30	0.7	32.5	18.0	67.5	2.59	0
NAB 10-40-50	10	40	50	0.7	20.4	17.8	79.6	2.65	0.18
NAB 20-40-40	20	40	40	2.0	55.6	18.5	44.4	2.61	0.30
NAB 60-30-10	60	30	10	1.6	20.1	18.8	79.9	2.69	0.14

Figure 4. 104.3 MHz  $^{27}\text{Al}$  MAS-NMR spectra of the  $\text{Na}_2\text{O}-\text{Al}_2\text{O}_3-\text{B}_2\text{O}_3$  glasses according to table 1; aluminum lactate as precursor species.

NMR parameters extracted from the spectra of figure 3. As previously discussed for melt prepared  $\text{Na}_2\text{O}-\text{Al}_2\text{O}_3-\text{B}_2\text{O}_3$  glasses, these  $^{11}\text{B}$  MAS-NMR spectra allow a quantitative distinction between different kinds of local boron environments [6 and 7]. In the present system the local structure of B is dominated by three-coordinated  $\text{BO}_{3/2}$  units with an abundance of mostly  $> 90\%$  ( $\delta_{\text{iso}} \approx 18$  ppm) and only minor amounts of  $< 10\%$  of tetrahedrally bound  $\text{BO}_{4/2}$  groups are visible ( $\delta_{\text{iso}} = 1$  to 3 ppm). Furthermore, the present glasses appear to contain no asymmetric  $\text{BO}_{2/2}(\text{O}^-)$  units, in distinct contrast to the situation in the melt prepared glasses [6].

The  $^{27}\text{Al}$  MAS-NMR spectra, see figure 4, show three partially resolved signals with resonance shifts (uncorrected for second-order quadrupolar effects) between 62 to 68, 36 to 38, and 5 to 9 ppm which are assigned to four-, five-, and six-coordinated aluminum species, respectively. While four-coordinated Al dominates for most of the compositions investigated, the fractions of five- and six-coordinated Al appear to be increased significantly in comparison to the melt cooled materials [6].

Two of the sol-gel glasses investigated display particular anomalies in the NMR spectra, namely composition NAB 11 with a high  $N_4$  value of 17.2 %, see table 1, and a missing portion of six-coordinated Al, see figure 4, and composition NAB 25 with the sharp and pronounced  $^{27}\text{Al}$  resonance near 60 ppm suggesting partial crystallization. The reasons for these deviations are not yet fully understood; possibly they originate from differences during the drying processes which change the thermal histories of the materials.

Figures 5 and 6 summarize the  $^{11}\text{B}$  and  $^{27}\text{Al}$  MAS-NMR spectra of the aluminum formiate based sol-gel glasses measured in the present study. Table 2 contains the corresponding  $^{11}\text{B}$  NMR parameters extracted from the spectra of figure 5. Contrary to the results in table 1 for the aluminum lactate-based sol-gel glasses the present glasses show in most cases local structures with about 60 %  $\text{BO}_{3/2}$  and about 40 %  $\text{BO}_{4/2}$  units. However, as in the case of the lactate based sol-gel glasses the present glasses also do not appear to contain  $\text{BO}_{2/2}(\text{O}^-)$  units. Most of the  $^{27}\text{Al}$  NMR spectra in figure 6 reveal, similar to the results of the lactate

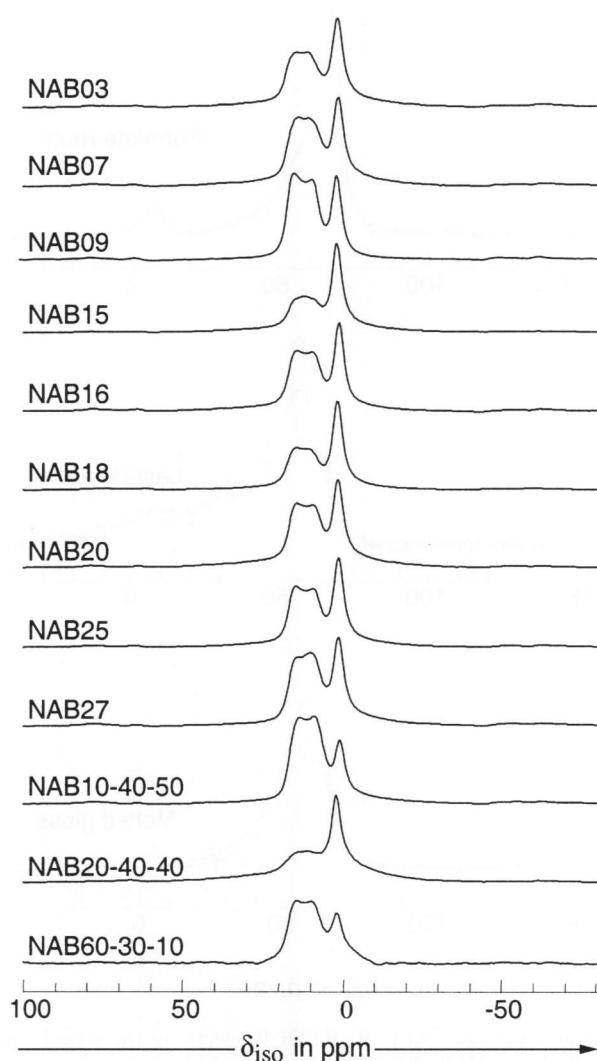


Figure 5. 160.4 MHz <sup>11</sup>B MAS-NMR spectra of the Na<sub>2</sub>O–Al<sub>2</sub>O<sub>3</sub>–B<sub>2</sub>O<sub>3</sub> glasses according to table 2; aluminum formiate as precursor species.

based glasses, Al in four-, five- and sixfold coordination, however, with a much higher portion of the latter coordination state. Some sol-gel glasses such as NAB 15 and NAB 20-40-40 have a lower portion of BO<sub>3/2</sub> units and more Al in sixfold coordination. A similar tendency of more Al in sixfold coordination holds also for glass NAB 18, whereas NAB 27 displays the opposite tendency, a much higher degree of Al in tetrahedral surroundings. Possibly these anomalies may also depend on the drying conditions which sensitively can influence the thermal histories and hence the local structures of the materials.

Figures 7a to c and 8a to c show the <sup>11</sup>B {<sup>27</sup>Al} and <sup>27</sup>Al {<sup>11</sup>B} REDOR results for a representative composition (NAB 09). The upper curves are regular MAS NMR spectra, whereas the lower ones are the spectra obtained with partial heterodipolar dephasing during an evolution time of 1 ms. The signal attenuation observed relative to the respective top spectrum is a consequence of heteronuclear <sup>11</sup>B–<sup>27</sup>Al dipole-dipole interactions which arise as a consequence of spatial proximity of the two types of nuclei. Thus, the intensity difference between both spectra can be taken as a semi-quantitative measure of the extent of B–O–Al

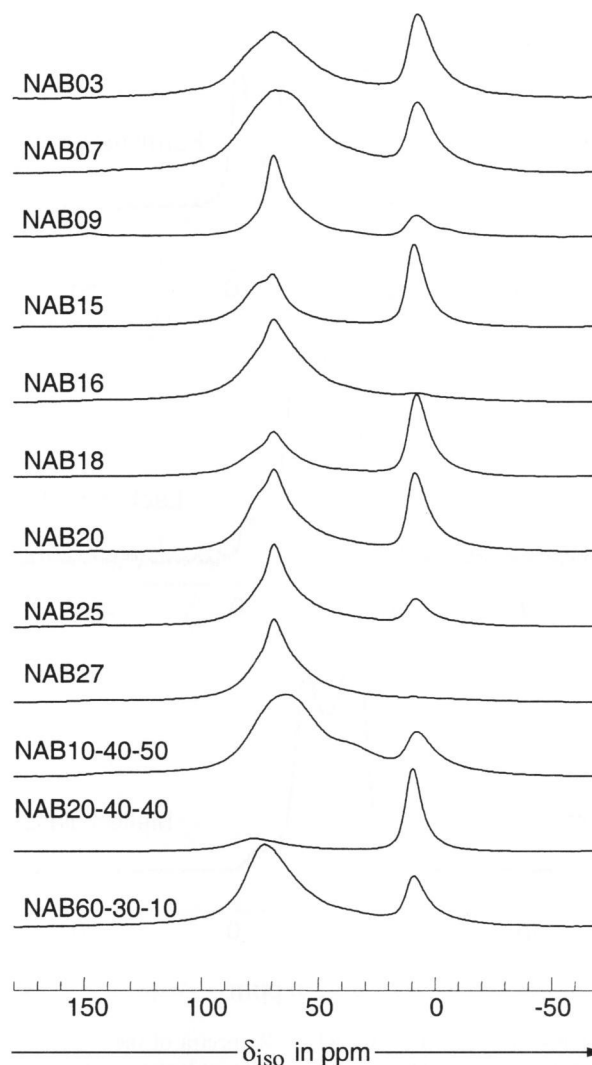
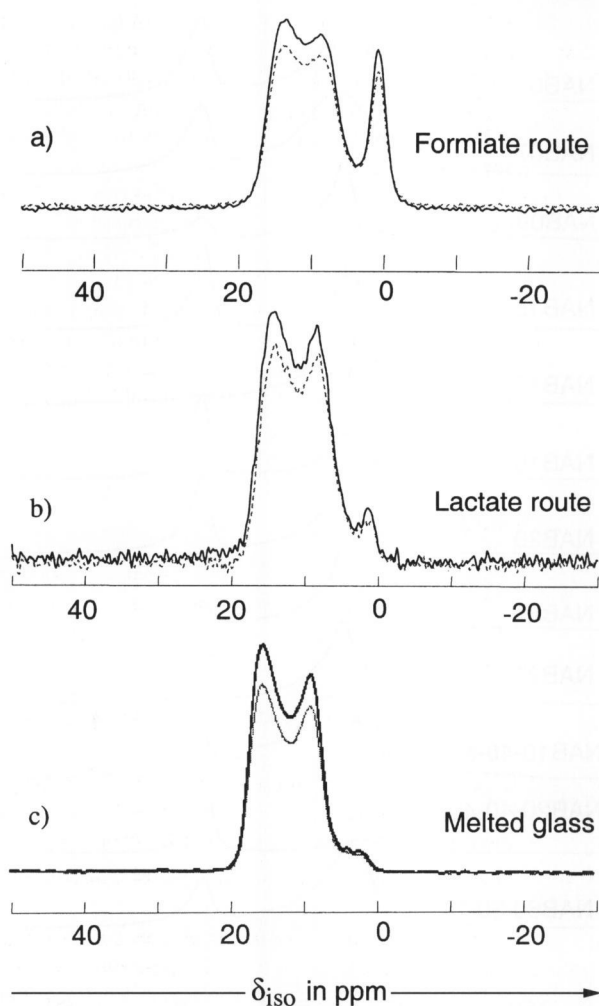


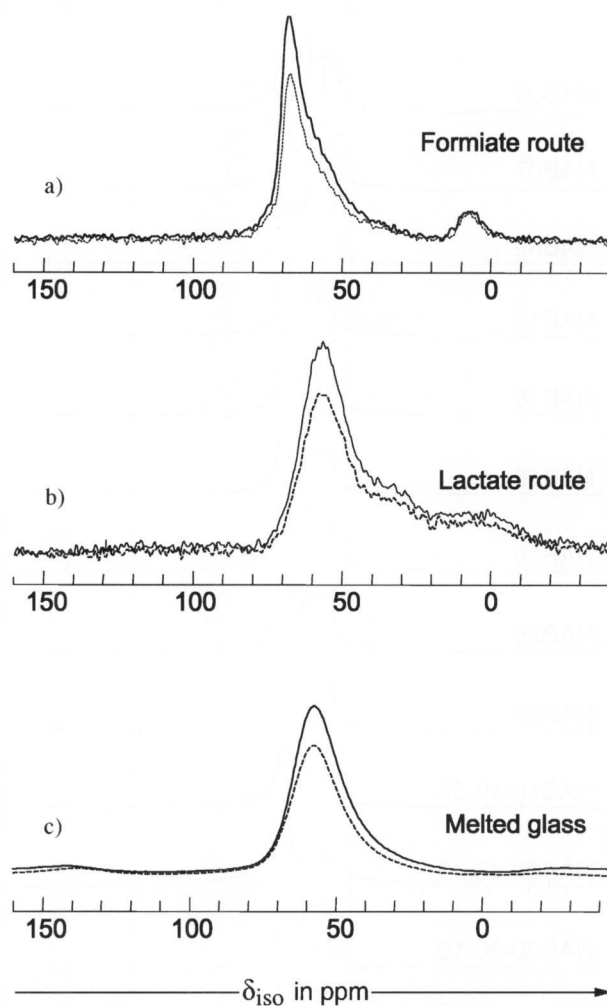
Figure 6. 130.8 MHz <sup>27</sup>Al MAS-NMR spectra of the Na<sub>2</sub>O–Al<sub>2</sub>O<sub>3</sub>–B<sub>2</sub>O<sub>3</sub> glasses according to table 2; aluminum formiate as precursor species.

connectivity. The results indicate in general that in the glasses prepared via all three preparation routes the <sup>11</sup>BO<sub>3/2</sub> units are more strongly connected to aluminum than the <sup>11</sup>BO<sub>4/2</sub> units. In addition, the <sup>27</sup>AlO<sub>4</sub> groups show significantly stronger dipolar interactions with <sup>11</sup>B than the <sup>27</sup>AlO<sub>5</sub> or the <sup>27</sup>AlO<sub>6</sub> units present. Overall, the results of figures 7a to c and 8a to c, as well as similar results obtained on other glasses suggest that the extent of B–O–Al connectivity in the gel prepared glasses is somewhat diminished compared to the situation in the melt cooled glasses.

A comparison of the glasses obtained by the three different preparation routes, aluminum lactate, aluminum formiate and melt cooling, indicates that the mode of preparation has a significant influence on the local structure of the Na<sub>2</sub>O–Al<sub>2</sub>O<sub>3</sub>–B<sub>2</sub>O<sub>3</sub> glasses. This holds with respect to the abundance of the BO<sub>3/2</sub>, BO<sub>4/2</sub>, and BO<sub>2/2</sub>(O<sup>−</sup>) units and also with the differing portions of Al in four-, five- and sixfold coordination. These findings are in marked contrast to the situation in Na<sub>2</sub>O–Al<sub>2</sub>O<sub>3</sub>–P<sub>2</sub>O<sub>5</sub> and Al<sub>2</sub>O<sub>3</sub>–P<sub>2</sub>O<sub>5</sub> glasses, where the aluminum lactate sol-gel route and the melt-cooling process produced glasses with essentially identical local structures [3 and 4]. The REDOR data also reveal



Figures 7a to c.  $^{11}\text{B}$  { $^{27}\text{Al}$ } REDOR spectra of the sol-gel and melt glasses NAB 09; a) formiate route, b) lactate route, and c) melted glass.



Figures 8a to c.  $^{27}\text{Al}$  { $^{11}\text{B}$ } REDOR spectra of the sol-gel and melt glasses NAB 09; a) formiate route, b) lactate route, and c) melted glass.

significant differences. Whereas in the case of the  $\text{Na}_2\text{O}-\text{Al}_2\text{O}_3-\text{P}_2\text{O}_5$  glasses the P-O-Al connectivity is maximized [3], evidencing a tight glass network, the  $\text{Na}_2\text{O}-\text{Al}_2\text{O}_3-\text{B}_2\text{O}_3$  glasses tend to present a diminished extent of B-O-Al connectivity. This result points towards partially independent B-O and Al-O structural sub-networks in the gel prepared materials.

### 3.2 SNMS and AFM data

Figure 9 displays SNMS in-depth profiles from the surface into a thick film of a lactate based sol-gel glass sample of composition NAB 03, plotted as intensity versus sputter time. Apart from the very surface the major constituents are practically constant up to a depth of about 1000 nm, showing a good elemental homogeneity of this material. The carbon profile reveals a minor enrichment towards the surface; however, its overall content is so low that visually no greyish coloration of the glasses can be evidenced. Similar results were also obtained for other compositions and also for the formiate based materials, except for some minor relative enrichment or depletion of several constituents, e. g. Na, near the surfaces [10]. It is well known that due to weathering

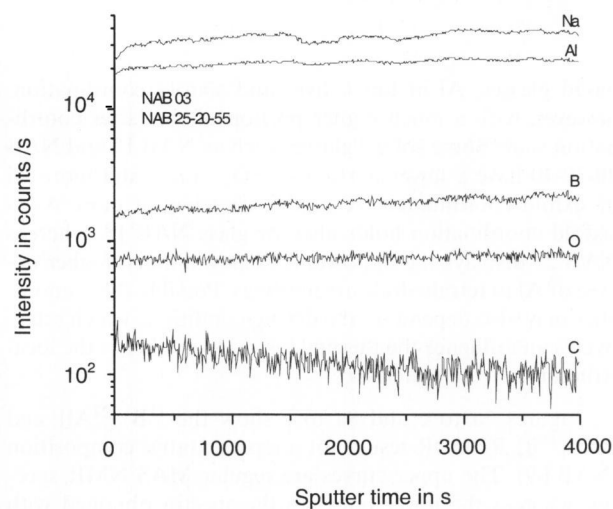


Figure 9. SNMS in-depth profiles of the sol-gel glass NAB 03; aluminum lactate as precursor.

during preparation, storage and handling, respectively, glass surfaces may be attacked more or less strongly and deviations in the concentration profiles are evident [11]. An es-

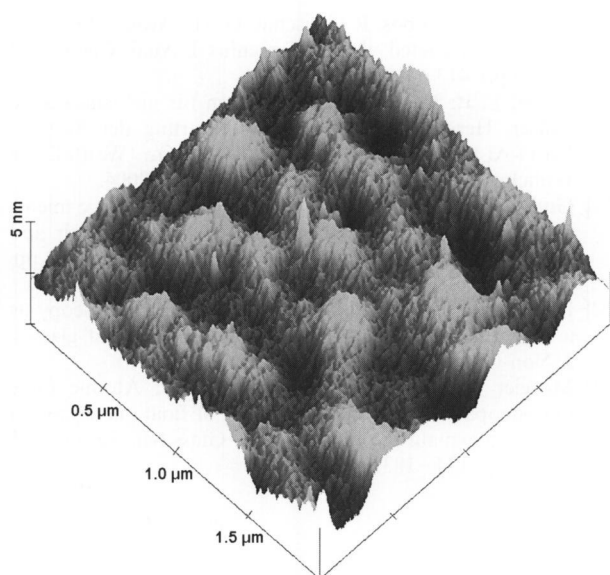


Figure 10. AFM image of the surface of the sol-gel glass NAB 03; aluminum formiate as precursor.

sential result is the low carbon content of all the samples approaching the detection limit of the analysis method. It shows that this constituent is practically fully removed. This process is greatly enhanced by the use of the short-chain organic precursors which during their decomposition generate highly volatile constituents. The formiate ions are known to be easily oxidized and formamide forms pores which also facilitate this removal. These pores can be observed already with an optical microscope. An SNMS analysis of the melted glass reveals similar results, however, due to its higher density (no pores) it has a somewhat differing sputtering response. The carbon content at the surface results from impurities; in the compact bulk it is even a little lower than in the sol-gel glasses.

The porosity of the gel prepared glasses is also clearly evidenced on the AFM image in figure 10. The  $x, y$  scales are in total 2  $\mu\text{m}$  each, the  $z$  scale is divided into 5 nm steps. One can see the irregular ripple pattern common to glass surfaces and also to surfaces of glassy sol-gel coatings [9 and 12]. The average ripple diameter is  $\bar{d} = 136$  nm and the average ripple height amounts to  $\bar{h} = 0.7$  nm. The root mean square roughness (rms) of the  $z$  values is 0.4 nm, related to an area of  $(1 \times 1) \mu\text{m}^2$ . The data for technical float glass surfaces are 60 nm,  $< 1$  and  $< 0.25$  nm, fracture surfaces are coarser and show values of 90 to 140, 1 to 2, and 0.6 to 0.8 nm, respectively [13]. In the present case there are surfaces nearly as smooth as those of float glass, though there are also examples of much coarser surfaces. Previous investigations on the nanostructures of coatings display in some cases also a rougher pattern [12]. However, further reasons can also be seen in a sensitive corrosion process by the ambient water vapor [11] and/or an etching by substances like acetic anhydride or formiate, leading to higher roughness values. This holds also for the melt formed glasses.

Compared to the standard melting route the sol-gel process is a low-temperature alternative for the preparation of glasses. A comparison of the ranges of composition, see tables 1 and 2, to the area of glass formation by the melting

process [6] displays that the sol-gel method can lead even to glassy materials outside the melt area, see compositions NAB 10-40-50, NAB 20-40-40, and NAB 60-30-10 of table 2. This is known also for other glass forming systems and may be understood by the fact that due to the low processing temperatures crystallization and phase separation processes do not play such an important role as during high-temperature melting [1 and 2]. On the other hand it could be clearly shown for the system Na<sub>2</sub>O–Al<sub>2</sub>O<sub>3</sub>–B<sub>2</sub>O<sub>3</sub> investigated in this work that the local structures of the glassy materials strongly depend on the route of preparation, whether one uses aluminum lactate or aluminum formiate as precursors in the sol-gel process or the high-temperature melting route. Of course, this dependence should also influence the properties of these materials.

#### 4. Conclusions

Sol-gel glasses of the non-silicate system Na<sub>2</sub>O–Al<sub>2</sub>O<sub>3</sub>–B<sub>2</sub>O<sub>3</sub> have been prepared using aluminum lactate and aluminum formiate as precursors. The methodology to obtain stable sols, gels and, after annealing, transparent glasses is described. The most important findings, applying solid-state NMR, SNMS, and AFM investigations, are as follows:

- the <sup>11</sup>B spectra show the presence of BO<sub>3/2</sub> and BO<sub>4/2</sub><sup>-</sup> units in the glasses; however, asymmetric B<sub>2/2</sub>(O<sup>-</sup>) units as found in melt quenched glasses could not be evidenced;
- the <sup>27</sup>Al spectra show Al in four-, five-, and sixfold coordination;
- a comparison of the local atomic structures displays that these strongly depend on the precursors and the route of preparation, and they differ also from the local atomic structures found earlier for melt prepared glasses;
- REDOR results suggest that the extent of B–O–Al connectivity in the gel prepared glasses tends to be weaker than in the melt prepared glasses;
- the sol-gel routes are capable of preparing glasses well outside the glass forming area by melting;
- the SNMS in-depth profiles reveal elemental homogeneity, and the AFM investigations show a surface nanostructure consisting of an irregular ripple pattern.

\*

The authors thank the Deutsche Forschungsgemeinschaft, Bonn, for financial support through grants FR 273/54-3 and EC168/4-3 within the cooperative programme "Vom Molekül zum Material". They are also grateful to Dipl.-Ing. T. Peter, TU Clausthal, for the SNMS measurements, and Prof. Dr. E. Rädlein, Universität Bayreuth, for an extensive discussion of the AFM results.

#### 5. References

- Beier, W.: Glasbildung und Glasstruktur unter besonderer Berücksichtigung des Alkoxid-Gelverfahrens. Technische Universität Clausthal, habilitation thesis, 1989.
- Brinker, C. J.; Scherrer, G. W.: Sol-Gel-Science. Boston et al.: Academic Press, 1990.
- Zhang, L.; Chan, J. C. C.; Eckert, H. et al.: A novel sol-gel synthesis of sodium aluminophosphate glass based on aluminum lactate. Chem. Mat. **15** (2003) pp. 2702–2710.

- [4] Zhang, L.; Eckert, H.; Hensch, G. et al.: Aluminum lactate = an attractive precursor for the sol-gel synthesis of alumina-based glass. In: Proc. XX International Congress on Glass, Kyoto 2004. 7 pp.
- [5] Zhang, L.; Eckert, H.; Hensch, G. et al.: Network modification of glassy AlPO<sub>4</sub>: Sol-gel synthesis and structural characterization of the system Na<sub>2</sub>O–AlPO<sub>4</sub>. *Z. Phys. Chem.* **219** (2005) pp. 71–87.
- [6] Züchner, L.; Chan, J. C. C.; Müller-Warmuth, W. et al.: Short-range order and site connectivities in sodium aluminoborate glasses: I. Quantification of local environments by high-resolution <sup>11</sup>B, <sup>23</sup>Na, and <sup>27</sup>Al solid-state-NMR. *J. Phys. Chem.* **B102** (1998) pp. 4495–4506.
- [7] Bertmer, M.; Züchner, L.; Chan, J. C. C. et al.: Short-range order and site connectivities in sodium aluminoborate glasses: II. Site connectivities and cation distributions studied by rotational echo double resonance NMR spectroscopy. *J. Phys. Chem.* **B104** (2000) pp. 6541–6553.
- [8] Ambos, R.; Rädlein, E.; Frischat, G. H.: Surface analysis of sol-gel coatings on glass by secondary neutral mass spectrometry. *Fresenius J. Anal. Chem.* **353** (1995) pp. 614–618.
- [9] Rädlein, E.; Ambos, R.; Frischat, G. H.: Atomic force microscopy of coated glasses. *Fresenius J. Anal. Chem.* **353** (1995) pp. 413–418.
- [10] Hoyer, L. P.: Neue Sol-Gel-Verfahren für nichtsilicatische Gläser. Herstellung und Charakterisierung der Systeme Na<sub>2</sub>O–Al<sub>2</sub>O<sub>3</sub>–P<sub>2</sub>O<sub>5</sub> und Na<sub>2</sub>O–Al<sub>2</sub>O<sub>3</sub>–B<sub>2</sub>O<sub>3</sub>. Westfälische Wilhelms-Universität Münster, PhD thesis, 2004.
- [11] Goß, A.; Rädlein, E.; Frischat, G. H.: Atomic force microscope study of silicate glass fracture surfaces in air and water environment. *Glass Sci. Technol.* **76** (2003) pp. 244–251.
- [12] Rädlein, E.; Frischat, G. H.: Atomic force microscopy as a tool to correlate nanostructure to properties of glasses. *J. Non-Cryst. Solids* **222** (1997) pp. 69–82.
- [13] Moseler, D.; Heide, G.; Frischat, G. H.: Atomic force microscope study of the topography of float glasses and a model to explain the bloom effect. *Glass Sci. Technol.* **75** (2002) pp. 174–183.

■ E405P005

## Contact:

Prof. Dr. G. H. Frischat  
Institut für Nichtmetallische Werkstoffe  
Technische Universität Clausthal  
Zehntnerstraße 2A  
D-38678 Clausthal-Zellerfeld  
E-mail: guenther.frischat@tu-clausthal.de